ACS OMEGA

Open Access

http://pubs.acs.org/journal/acsodf

Article

Polymorphs of Substituted *p*-Toluenesulfonanilide: Synthesis, Single-Crystal Analysis, Hirshfeld Surface Exploration, and Theoretical Investigation

Mehreen Riaz, Akbar Ali,* Muhammad Ashfaq, Muhammad Ibrahim, Nadia Akram, Muhammad Nawaz Tahir, Aleksey Kuznetsov, Lyanne Rodríguez, Manal Y. Sameeh, Mohammed A. Assiri, and Alexander Fernandez de la Torre*

Cite This: *ACS Omega* 2023, 8, 35307−35320

Read Online

ACCESS | Metrics & More | Article Recommendations | Supporting Information

ABSTRACT: Polymorphism is an exciting feature of chemical systems where a compound can exist in different crystal forms. The present investigation is focused on the two polymorphic forms, triclinic (**MSBT**) and monoclinic (**MSBM**), of ethyl 3-iodo-4-((4-methylphenyl)sulfonamido)benzoate prepared from ethyl 4-amino-3-iodobenzoate. The prepared polymorphs were unambiguously confirmed by single-crystal X-ray diffraction (SC-XRD) analysis. According to the SC-XRD results, the molecular configurations of both structures are stabilized by intramolecular N−H···I and C−H···O bonding. The crystal packing of **MSBT** is different as compared to the crystal packing of **MSBM** because **MSBT** is crystallized in the triclinic crystal system with the space group $P\bar{1}$, whereas **MSBM** is crystallized in the monoclinic crystal system with the space group $P2_1/c$. The molecules of **MSBT** are interlinked in the form of dimers through N−H···O bonding to form $R_2^2(8)$ loops, while the **MSBM** molecules are connected with each other in the form of an infinite chain through C−H···O bonding. The crystal packing of both compounds is further stabilized by off-set $\pi\cdots\pi$ stacking interactions between phenyl rings, which is found stronger in **MSBM** as compared to in **MSBT**. Moreover, Hirshfeld surface exploration of the polymorphs was carried out, and the results were compared with the closely related literature structure. Accordingly, the supramolecular assembly of these polymorphs is mainly stabilized by noncovalent interactions or intermolecular interactions. Furthermore, a density functional theory (DFT) study was also carried out, which provided good support for the SC-XRD and Hirshfeld studies, suggesting the formation of both intramolecular and intermolecular interactions for both compounds.

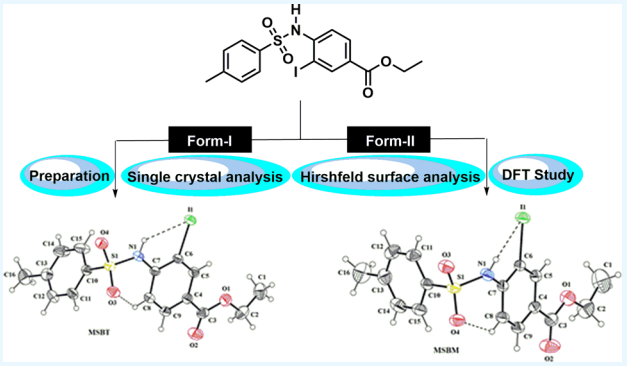

1. INTRODUCTION

Polymorphism from the crystallographic perspective is the capability of a particular compound to be present in different crystallographic forms due to the different packing aggregations of its molecules in the crystal structure.[1] However, it is important to mention that polymorphism and allotrophism are two different phenomena, i.e., allotropes mean the existence of different crystal structures of the same element, whereas polymorphism is the presence of different crystalline structures of the same compounds.[2] Polymorphism is an interesting structural phenomenon with great potential in the field of material science, since, although composed of the same compound, different polymorphs can behave as different materials having different physical, mechanical, and chemical properties.[3] Polymorphs have a key role in the commercialization and production of crystalline materials as agrichemicals, pharmaceuticals, food, pigments, and additives. Polymorphism also has an important role in fundamental research in order to help researchers to understand some basic chemical aspects of inter- and intramolecular interactions, the inducing forces pivoting the polymorphs' existence, and their structural repercussions.[4] Many organic compounds have shown the polymorphism phenomenon; among them, aniline derivatives are important to mention. One example is the existence of *N*-(4-methyl-2-nitrophenyl)acetamide in six polymorphic forms having different angles and axes as well as different densities, i.e., monoclinic with space group $P2_1/c$,[5] triclinic with space group P1 and monoclinic with space group $P2_1/c$,[6] monoclinic with space group $P2_1/c$,[7] monoclinic with space group $P2_1/c$,[8]

Received: July 16, 2023
Accepted: September 7, 2023
Published: September 15, 2023

https://doi.org/10.1021/acsomega.3c04957
ACS Omega 2023, 8, 35307−35320

Scheme 1. Preparation of Ethyl 3-iodo-4-((4-methylphenyl)sulfonamido)benzoate from Ethyl 4-amino-3-iodobenzoate and *p*-Toluenesulfonyl Chloride

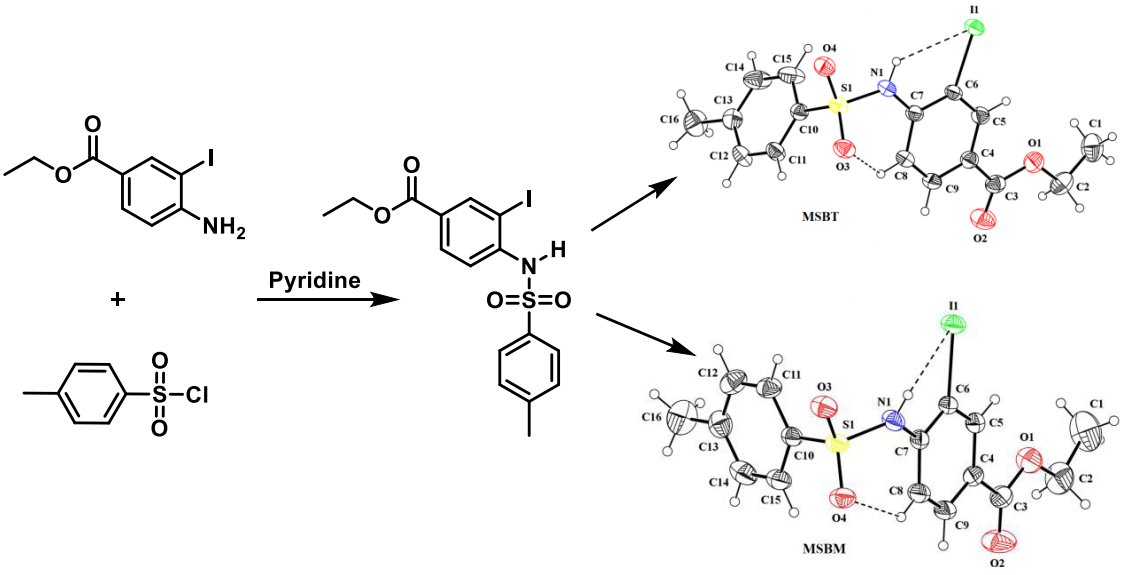

and triclinic with space group P1.[9] Similarly, 5-methyl-2-((2-nitrophenyl)amino)thiophene-3-carbonitrile has numerous polymorphic forms.[10] 2-((2-Nitrophenyl)amino)-3-thiophenecarbonitrile is one more organic compound existing in two crystalline forms, i.e., monoclinic and triclinic.[11] The well-known vitamin nicotinamide has also been reported as a highly polymorphic compound with nine solved single-crystal chemical structures.[12] Traditionally, the phenomenon of polymorphism has been observed in aromatic sulfonamide derivatives. Nangia et al. have investigated several substituted aromatic sulfonamides to be present in two or more crystal systems.[13] The orientation of the sulfonamide group has been observed to have a key role in poising the shape of the crystal, e.g., bis(p-tolyl) ketone p-tosylhydrazone could be observed in three conformational polymorphic forms, where one out of three polymorphs has an N−H···O═S dimer synthon, participating in hydrogen bonding, while this type of interaction is missing in the other two polymorphic forms.[14] In this context, Isao Azumaya et al. observed that the presence of halogen in the aromatic sulfonamides can induce polymorphism in the system as they investigated a series of aromatic sulfonamides and found that aromatic sulfonamides having a fluorine group can exist in more than one crystalline form, i.e., they show polymorphism as compared to aromatic sulfonamides that do not have the fluorine group.[15]

Density functional theory is an important tool for the exploration of key electronic features of organic compounds such as noncovalent interactions and charges etc.[16] The noncovalent interactive capacity of organic compounds predicted by DFT calculations plays a significant role in the pharmacological potential of these chemical building blocks.[17] Hirshfeld surface analysis is an attractive tool for finding out the types of intermolecular interactions to understand the stacking of molecular structures, density, mechanics, energy, and sensitivity.[18] Herein, we are reporting our findings regarding the preparation, DFT study, and X-ray and Hirshfeld studies of crystal packing of the two polymorphs of ethyl 3-iodo-4-((4-methylphenyl)sulfonamido)benzoate that are triclinic with the space group $P\bar{1}$ (**MSBT**) and monoclinic with the space group $P2_1/c$ (**MSBM**).

2. MATERIALS AND METHODS

Ethyl 3-iodo-4-((4-methylphenyl)sulfonamido)benzoate was prepared by the reaction of ethyl 4-amino-3-iodobenzoate and p-toluenesulfonyl chloride. Solvent purification was achieved by a simple distillation. To monitor reaction progress, a precoated silica gel aluminum sheet was used to perform thin-layer chromatography. The SC-XRD data were collected using the Bruker Kappa Apex-II diffractometer employing Mo Kα radiation and using Apex-II software,[19] whereas SAINT software was used for data integration.[20] SHEXS-97 software was used[21] for structure solutions, whereas data refinement was done using SHEXL 2018/3.[22] For graphical illustrations, PLATON,[23] Mercury 4.0,[24] and ORTEP-3[25] visualization programs were employed.

3. SYNTHESIS AND CRYSTALLIZATION

The substituted p-toluenesulfonanilide was prepared from substituted aniline according to procedure reported in the literature.[26] Accordingly, to a solution of ethyl 4-amino-3-iodobenzoate (2.3 mmol, 1 equiv) in pyridine (10 mL) was added p-toluenesulfonyl chloride (2.42 mmol, 1.05 equiv). The reaction mixture was stirred at room temperature for 2 h and then quenched with water (10 mL). The solution was extracted with DCM and the organic layer was washed with 10% aqueous $CuSO_4$ and then dried with anhydrous Na_2SO_4. After concentration with a rotary evaporator, the crude product was purified via column chromatography using 25% EtOAc/hexanes to yield the corresponding ethyl 3-iodo-4-((4-methylphenyl)sulfonamido)benzoate. The obtained compound was recrystallized in ethanol and was filtered before complete evaporation of the solvent. However, on close observation, two types of crystals were found, which were separated by applying the "Pasteur" manual method. Both types of crystals were subjected to single-crystal X-ray diffraction, which confirmed the triclinic form with the space group $P\bar{1}$ (**MSBT**) and the monoclinic form with the space group $P2_1/c$ (**MSBM**) (Scheme 1).

3.1. NMR Characterization of Ethyl 3-iodo-4-((4-methylphenyl)sulfonamido)benzoate. ^{1}H NMR (400

https://doi.org/10.1021/acsomega.3c04957
ACS Omega 2023, 8, 35307−35320

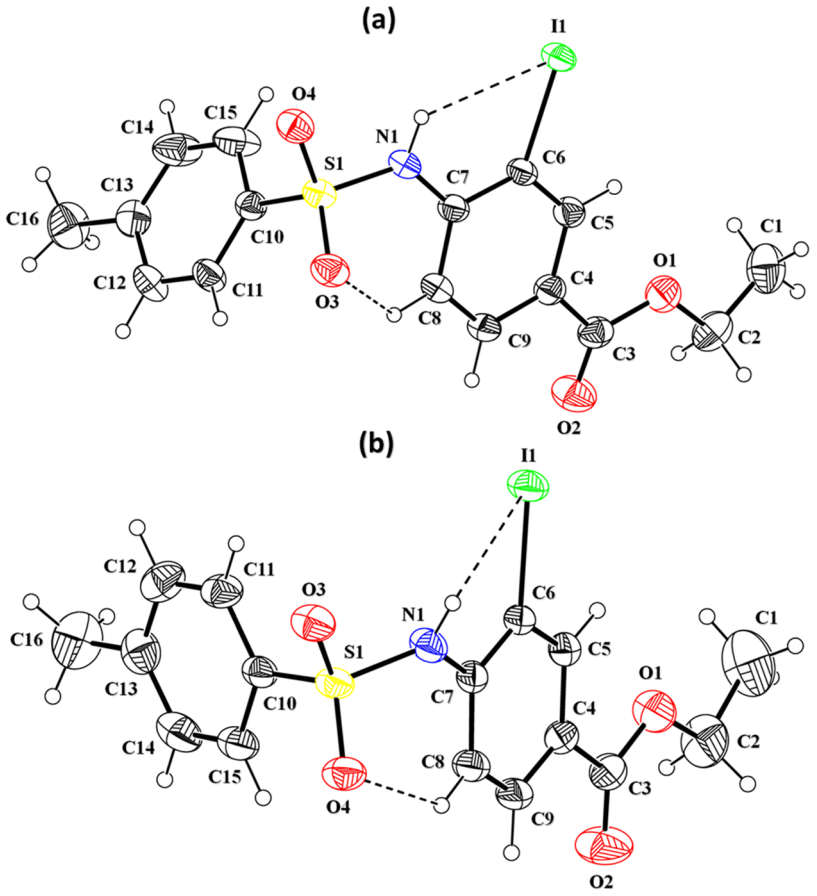

Figure 1. ORTEP diagrams of **MSBT** (a) and **MSBM** (b) drawn at the 30% probability level. Small circles of arbitrary radii represent H atoms.

MHz, $CDCl_3$) δ: 8.42 (d, J = 1.1 Hz, 1H), 8.32 (d, J = 8.5 Hz, 1H), 7.98 (d, J = 8.6 Hz, 1H), 7.69 (s, 1H), 4.35 (q, J = 7.1 Hz, 2H), 2.27 (s, 3H), 1.39 (t, J = 7.1 Hz, 3H). ^{13}C NMR (101 MHz, CDCl3) δ: 168.4, 164.6, 141.9, 140.1, 130.6, 127.4, 120.4, 88.6, 61.2, 24.9, 14.3.

4. DFT STUDIES

The computational study was done using the Gaussian 16 package.[27] To evaluate some specific properties of the compounds studied, we performed single-point calculations using the XRD structures of **MSBT** and **MSBM**. In these calculations, we used the hybrid functional B3LYP[28] along with the combination of the basis set of Ahlrichs and co-workers def2-TZVP for C, H, S, O, and N[29,30] and the 3-21G* basis set for I.[31] The calculations were performed with implicit effects from ethanol taken into account (dielectric constant ε-(C_2H_5OH) = 24.852) using the self-consistent reaction field IEF-PCM method[32] as implemented in Gaussian 16, with the UFF default model with the electrostatic scaling factor α set to 1.0. The charge analysis and the donor−acceptor stabilization energy analysis were performed using the natural bond orbital (NBO) approach as implemented in the Gaussian 16 package.[33] Moreover, molecular electrostatic potential (MEP) plots were calculated and analyzed. Molecular structures and MEP plots were visualized using Avogadro visualization software, version 1.1.1.[34,35]

5. RESULTS AND DISCUSSION

5.1. Exploration of the Crystal Structures of MSBT and MSBM. SC-XRD characterization was performed for both crystal systems, where the Cambridge Structural Database confirmed the novelty of these polymorphs. Table 1 provides experimental details related to SC-XRD.

In **MSBT** (Figure 1, Table 1), the ethyl formate group A (C1−C3/O1/O2) is roughly planar with a root-mean-square (rms) deviation of 0.1252 Å, whereas the corresponding similar group in **MSBM** is almost planar with an rms deviation of 0.0206 Å. The 2-iodoanilinic group B (C4−C9/N1/I1) and the toluene group C (C10−C16) are planar, with rms deviations of 0.0467 and 0.0119 Å, respectively, in **MSBT**, whereas in **MSBM**, the rms deviations of the corresponding similar groups are 0.0095 and 0.0045 Å. Group B is twisted at dihedral angles of 9.56(3) and 89.4(8)° with respect to groups A and C, respectively, in **MSBT**. The corresponding dihedral angles are 3.31(3) and 76.9(9)° in **MSBM**. The dihedral angles indicate that group B has a larger twist with respect to groups A and C in **MSBT** as compared to in **MSBM**, but overall, both molecules (Figure 1a,1b) are nonplanar. The important bond lengths and bond angles of **MSBT** and **MSBM** are listed in Table 2, and it could be seen that there is no large difference between the values of similar bond lengths and bond angles. The molecular configurations of both structures are stabilized by intramolecular N−H···I and C−H···O bonding. S(5) and S(6) hydrogen-bonded loops are formed by N−H···I and C−H···O bonding, respectively (Figure 2). The crystal packing of **MSBT** is different as compared to the crystal packing of **MSBM** because **MSBT** is crystallized in the triclinic crystal system with the space group $P\bar{1}$, whereas **MSBM** is crystallized in the monoclinic crystal system with the space group $P2_1/c$. The molecules of **MSBT** are interlinked in the form of dimers

https://doi.org/10.1021/acsomega.3c04957
ACS Omega 2023, 8, 35307−35320

Table 1. Experimental Details of MSBT and MSBM

crystal data	MSBT	MSBM
CCDC	2237903	2237904
chemical formula	$C_{16}H_{16}INO_4S$	$C_{16}H_{16}INO_4S$
M_r	445.26	445.26
crystal system, space group	triclinic, $P\bar{1}$	monoclinic, $P2_1/c$
temperature (K)	296	296
a, b, c (Å)	8.8898 (7), 9.6929 (7), 10.5211 (7)	9.0358 (11), 10.0610 (11), 19.806 (2)
α, β, γ (deg)	106.183 (3), 93.105 (4), 91.467 (4)	90, 90.728 (4), 90
V (Å^3)	868.60 (11)	1800.4 (4)
Z	2	4
radiation type	Mo Kα	Mo Kα
μ (mm^{-1})	1.98	1.91
crystal size (mm)	0.38 × 0.34 × 0.28	0.38 × 0.28 × 0.24
data collection		
diffractometer	Bruker Kappa APEXII CCD	Bruker Kappa APEXII CCD
absorption correction	Multiscan (*SADABS*; Bruker, 2007)	Multiscan (*SADABS*; Bruker, 2007)
no. of measured, independent, and observed [$I \geq 2\sigma(I)$] reflections	7096, 3268, 2955	10816, 3472, 2841
R_{int}	0.036	0.040
$(\sin\theta/\lambda)_{max}$ (Å^{-1})	0.617	0.617
Refinement		
$R[F^2 \geq 2\sigma(F^2)]$, $wR(F^2)$, S	0.029, 0.089, 1.11	0.034, 0.108, 1.04
no. of reflections	3268	3472
no. of parameters	210	210
H atom treatment	H atom parameters constrained	H atom parameters constrained
$\Delta\rho_{max}$, $\Delta\rho_{min}$ (e Å^{-3})	0.46, −0.54	1.00, −0.90

Table 2. Selected Bond Lengths and Bond Angles (Å, °) in MSBT and MSBM

selected bond lengths in **MSBT**		selected bond lengths in **MSBM**	
I1−C6	2.094 (3)	I1−C6	2.107 (3)
S1−O3	1.426 (2)	S1−O4	1.424 (3)
S1−O4	1.433 (2)	S1−O3	1.436 (3)
S1−N1	1.634 (3)	S1−N1	1.652 (3)
S1−C10	1.756 (3)	S1−C10	1.741 (4)
O1−C3	1.333 (4)	O1−C3	1.323 (6)
O1−C2	1.449 (4)	O1−C2	1.453 (5)
O2−C3	1.195 (4)	O2−C3	1.189 (5)
N1−C7	1.404 (4)	N1−C7	1.413 (5)
selected bond angles in **MSBT**		selected bond angles in **MSBM**	
O3−S1−O4	119.64 (15)	O4−S1−O3	119.68 (18)
O3−S1−N1	109.32 (14)	O4−S1−N1	108.95 (18)
O4−S1−N1	103.10 (14)	O3−S1−N1	103.43 (17)
O3−S1−C10	107.96 (15)	O4−S1−C10	108.53 (18)
O4−S1−C10	108.81 (15)	O3−S1−C10	109.39 (18)
N1−S1−C10	107.39 (14)	N1−S1−C10	105.99 (18)
C3−O1−C2	116.7 (3)	C3−O1−C2	116.0 (4)
C7−N1−S1	126.5 (2)	C7−N1−S1	125.1 (3)
O1−C2−C1	108.0 (4)	O1−C2−C1	106.9 (5)
O2−C3−O1	123.6 (3)	O2−C3−O1	123.0 (4)
O2−C3−C4	124.0 (3)	O2−C3−C4	124.3 (4)
C8−C7−N1	122.7 (3)	C8−C7−N1	121.8 (4)
C6−C7−N1	119.4 (3)	C6−C7−N1	120.0 (3)
C11−C10−S1	120.1 (2)	C11−C10−S1	119.4 (3)
C15−C10−S1	119.3 (3)	C15−C10−S1	120.5 (3)

through N−H···O bonding to form the $R_2^2(8)$ loop, where the O atom is from the sulfonyl group. The dimers are further connected with each other through C−H···O bonding, where CH is from group A and the O atom of the sulfonyl group that is not involved in formation of the dimer acts as a H-bond acceptor (Figure 2). The CH of group C also acts as a H-bond donor for the carbonyl O atom of group A. The molecules of **MSBM** are connected with each other in the form of an infinite chain (C11) through C−H···O bonding carbonyl O atom of group A. In the case of **MSBM**, no intermolecular N−H···O bonding exists and also the sulfonyl O atoms and CH of group A are not involved in H-bonding. The crystal packing of both compounds is further stabilized by offset $\pi\cdots\pi$ stacking interactions between phenyl rings (C1−C6) of the symmetry-related molecules. Offset $\pi\cdots\pi$ stacking interactions are stronger in **MSBM** (Figure 3a) as compared to those in **MSBT** (Figure 3b). The intercentroid separations between the rings are 4.17 and 3.84 Å in **MSBT** and **MSBM**, respectively. The ring offsets are 2.126 and 1.373 Å in **MSBT** and **MSBM**, respectively (Table 3).

A Cambridge structural database (CSD 2022, updated September 2022) search is performed in order to find the related crystal structures of the literature. The search provides three crystal structures with the reference codes DAYWUW,[36] LANYEG,[37] and ODASAO[38] that have close similarity to the crystal structures of **MSBT** and **MSBM**. The above-mentioned related crystal structures have a toluene ring at one end but do not have an iodine atom. As compare to the crystal structure of the compound **MSBM**, the crystal structure of the related compounds are crystallized in the monoclinic crystal system but the space group of DAYWUW and LANYEG is $P2_1/n$. The dihedral angles between the phenyl rings are 88.18 (1) and 77.16 (1)° in **MSBT** and **MSBM**, respectively. The dihedral angles between the corresponding rings in the crystal structures of DAYWUW, LANYEG, and ODASAO are 93.4 (1), 88.05 (7), and 34.7 (1)°, respectively. The similarity in terms of crystal packing is that intermolecular N−H···O bonding is present in DAYWUW, LANYEG, and ODASAO. In DAYWUM, the molecules are stacked along the *b*-axis by N−H···O bonding, whereas in LANYEG, the three-dimensional network of molecules is formed by N−H···O and C−H···O bonding. In ODASAO, the molecules are connected in the form of a chain by N−H···O and O−H···O bonding that runs along the [011] direction.

5.2. Hirshfeld Surface Analysis. The exploration of the supramolecular assembly in single crystals is getting more and more attention from researchers and industrialists nowadays as the properties of single crystals depend on the way the molecules are packed together. The supramolecular assembly is mainly stabilized by the noncovalent interactions or intermolecular interactions. In this perspective, we are going to elaborate on the intermolecular interactions present in **MSBT** and **MSBM** by Hirshfeld surface analysis on Crystal Explorer version 21.5.[39] In order to make that analysis interesting for readers, we are going to compare the intermolecular interactions in **MSBT** and **MSBM** with the intermolecular interactions in the closely related crystal structure of the literature with the reference code **DAYWUW**. The concept of Hirshfeld surface emerged when the researchers were trying to divide the crystal density into molecular fragments. Hirshfeld surface can be formed by using a number of properties like normalized distances (d_{norm}), d_i, d_e, shape index, curvedness, etc. Information regarding the short

https://doi.org/10.1021/acsomega.3c04957
ACS Omega 2023, 8, 35307−35320

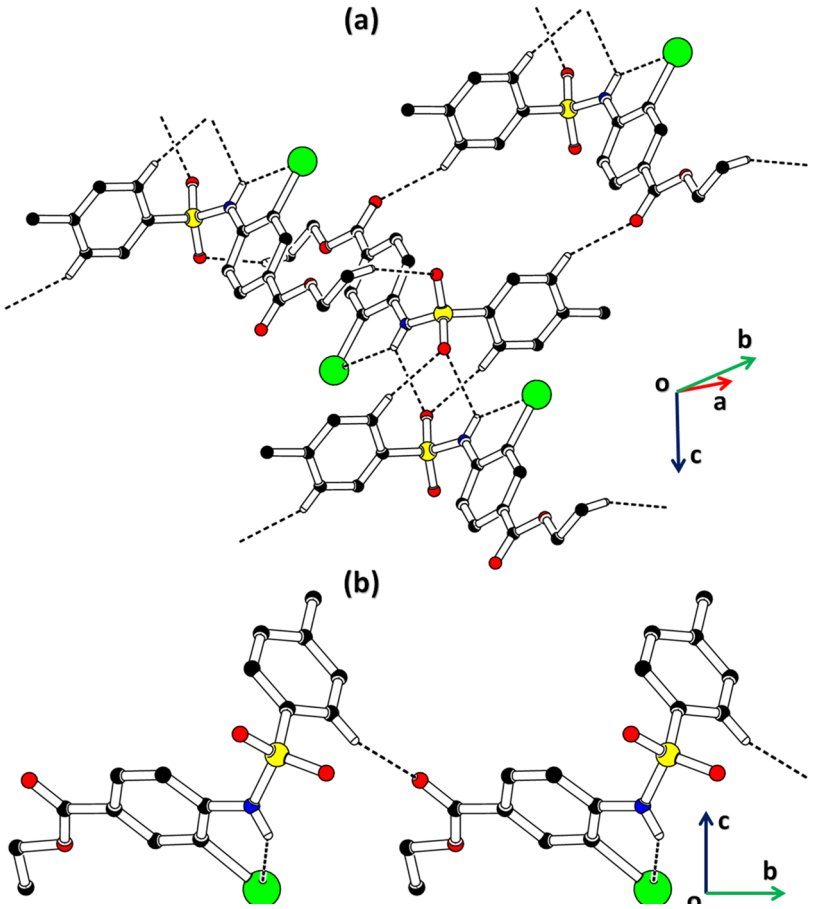

Figure 2. Packing diagram of (a) **MSBT** and (b) **MSBM**. Only selected H atoms are shown for clarity.

contacts can be extracted by the Hirshfeld surface plotted over d_{norm}[40−44]. The surface contained three colors: red, blue, and white. Red and blue spots on the surface showed short and long contacts, respectively. The contacts for which the distance between the atoms is equal to the sum of the van der Waal radii of the atoms are shown by white spots. The red around the NH group and O atoms of the sulfonyl group in the case of the Hirshfeld surface of **MSBT** (Figure 4a) showed that these atoms are involved in H-bonding interactions. Similarly, the red spot around the particular O atom of the sulfonyl group in the case of the Hirshfeld surface of **MSBM** (Figure 4b) showed its involvement in H-bonding. The red on the surface around the iodine atom in the case of **MSBT** showed a short I···I contact of 3.7903 (4) Å, whereas in **MSBM**, it showed a short I···O contact of 3.0618 (3) Å. The red spot around the NH group and the carbonyl O atom in the case of the Hirshfeld surface of **DAYWUW** (Figure 4c) showed their involvement in H-bonding interactions, but no red spot around sulfonyl O atoms inferred that these atoms play no significant role in stabilization of the crystal packing.

The intermolecular interactions that are weaker than the H-bonding interactions can be visualized and verified by plotting the Hirshfeld surface over the shape index. The presence of consecutive red and blue triangular-shaped regions around the aromatic ring is the conformation of its involvement in $\pi\cdots\pi$ stacking interactions. The above-mentioned regions are found on the surface of **MSBT**, **MSBM**, and **DAYWUW** (Figure 5a−c), verifying that $\pi\cdots\pi$ stacking interactions are present in these compounds. The presence of $\pi\cdots\pi$ stacking interactions in **MSBT**, **MSBM**, and **DAYWUW** is also confirmed by flat green regions around aromatic rings on the surface plotted over curvedness (Figure 5d−f).[45] The flat green regions are outlined by dashed circles and ellipses.

The overall interactions present in the single crystal can be fragmented in order to find the contribution of contacts in the crystal packing.[46−49] For that purpose, two-dimensional (2D) fingerprint plots are formed. Figure 6a,e,i shows the 2D plot of overall interactions in **MSBT**, **MSBM**, and **DAYWUW**, respectively. As each 2D plot of overall interaction has a unique shape, it is a clear indication that the same contacts in **MSBT**, **MSBM**, and **DAYWUW** have different contributions in the crystal packing. The interatomic and intermolecular contacts H···H, H···O, and H···C are the main contributors to the crystal packing in the cases of **MSBT**, **MSBM**, and **DAYWUW**. The contributions of H···H, H···O, and H···C contacts in the crystal packing of **MSBT** are 39.5, 23.9, and 16.3%, respectively (Figure 6b−d). The contributions of the corresponding contacts in **MSBM** are 36.8, 24.4, and 19.4%, respectively (Figure 6f−h), and in **DAYWUM**, they are 44.5, 27.5, and 22.9%, respectively (Figure 6j−k). Although the NH contacts are also important as there is NH−O bonding, the crystal structures of **MSBT**, **MSBM**, and DAYWUW possessed only one NH group, so the contribution of this contact is smaller as compared to the contribution of contacts shown in Figure 6. All pairs of chemical species present in the single crystal have a unique ability to be involved in intermolecular interactions. Some contacts have a higher tendency to form crystal packing interactions as compared to other contacts. The

https://doi.org/10.1021/acsomega.3c04957
ACS Omega 2023, 8, 35307−35320

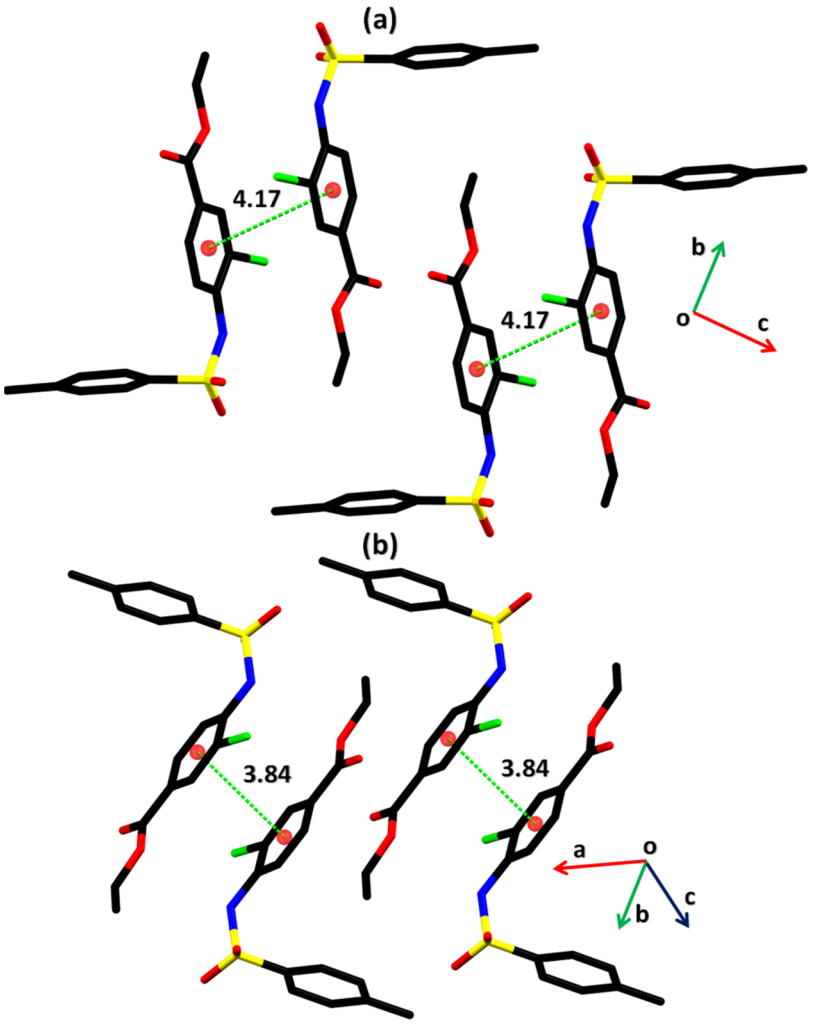

Figure 3. Graphical representation of offset $\pi\cdots\pi$ stacking interactions in (**a**) **MSBT** and (**b**) **MSBM**. H atoms are not shown for clarity. Distances are given in Å.

Table 3. Hydrogen-Bond Geometry (Å, °) in MSBT and MSBM[a]

MSBT	D−H···A	D−H	H···A	D···A	∠(D−H···A)°
	N1−H1···I1	0.86	2.70	3.225 (2)	121
	C8−H8···O3	0.93	2.48	3.086 (4)	123
	N1−H1···O4^{i}	0.86	2.55	3.114 (3)	124
	C1−H1*A*···O3^{ii}	0.96	2.55	3.469 (5)	160
	C15−H15···O4^{i}	0.93	2.49	3.380 (5)	160
MSBM	D−H···A	D−H	H···A	D···A	∠(D−H···A)°
	N1−H1···I1	0.86	2.86	3.237 (3)	108
	C8−H8···O4	0.93	2.41	3.064 (5)	127
	C11−H11···O2^{iii}	0.93	2.58	3.252 (5)	130

[a]Symmetry codes: (i) $-x + 1, -y + 1, -z + 1$; (ii) $-x + 1, -y, -z$; (iii) $x, y + 1, z$.

tendency of the pair to form a crystal packing interaction can be determined by the enrichment ratio.[50,51] The pair for which the enrichment ratio is greater than 1 has a higher tendency to form crystal packing interactions as compared to the other pairs. Tables S1−S3 show the enrichment ratio of the pairs of species in **MSBT**, **MSBM**, and **DAYWUW**. The most favorable contact in **MSBT** is C···I with enrichment ratio 1.64, whereas the most favorable contacts in **MSBM** and **DAYWUW** are C···O (with enrichment ratio 1.48) and N···H (with enrichment ratio 1.42), respectively (Figure 7).

The properties of a single crystal depend on the voids present in it. The crystal having no large cavities is expected to have better mechanical properties as compared to the crystal with large cavities. We calculate voids in **MSBT**, **MSBM**, and **DAYWUW** by using the Hartree−Fock theory.[52−54] According to this theory, all of the atoms are assumed to be spherically symmetric and electron densities of the atoms are summed for calculating voids. The volumes of voids are found to be 111.02, 282.15, and 205.68 Å^3 in **MSBT**, **MSBM**, and **DAYWUW**, respectively. The percentage spaces occupied by voids in **MSBT**, **MSBM**, and **DAYWUW** are 12.78, 15.67, and 13.02%, respectively. As the voids occupy a tiny space in the crystal packing of the compounds, it means that there is no large cavity in the compounds. The compounds are expected to have good mechanical properties like melting point, mechanical strength, etc.

In order to further explore the supramolecular assembly, we calculated the interaction energy between molecular pairs. The interaction energy between a molecular pair is the sum of four types of energies, named as Coulomb, repulsion, dispersion, and polarization.[55−58] The Coulomb energy can be attractive (negative) or repulsive (positive), whereas dispersion energy is

https://doi.org/10.1021/acsomega.3c04957
ACS Omega 2023, 8, 35307−35320

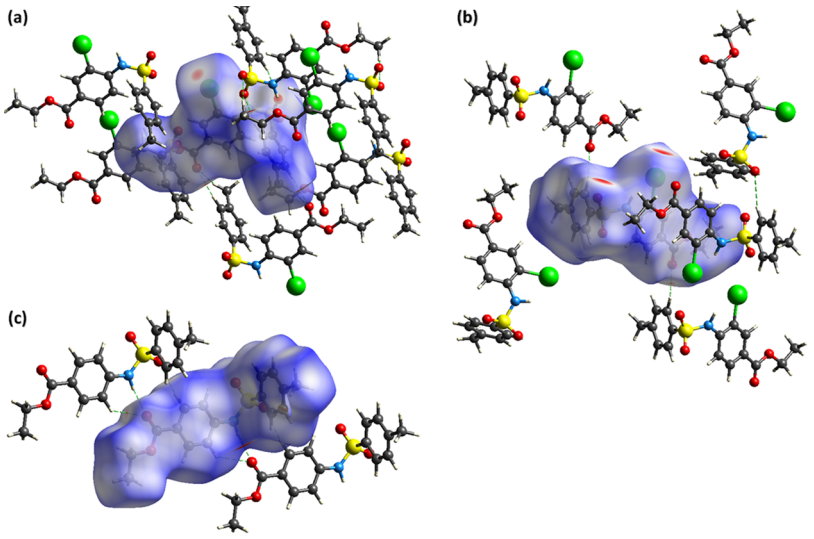

Figure 4. Hirshfeld surface plotted over for (**a**) **MSBT** in the range −0.1925 to 1.3289 au, (**b**) **MSBM** in the range −0.2598 to 1.4899 au, and (**c**) **DAYWUW** in the range −0.4971 to 1.2190 au.

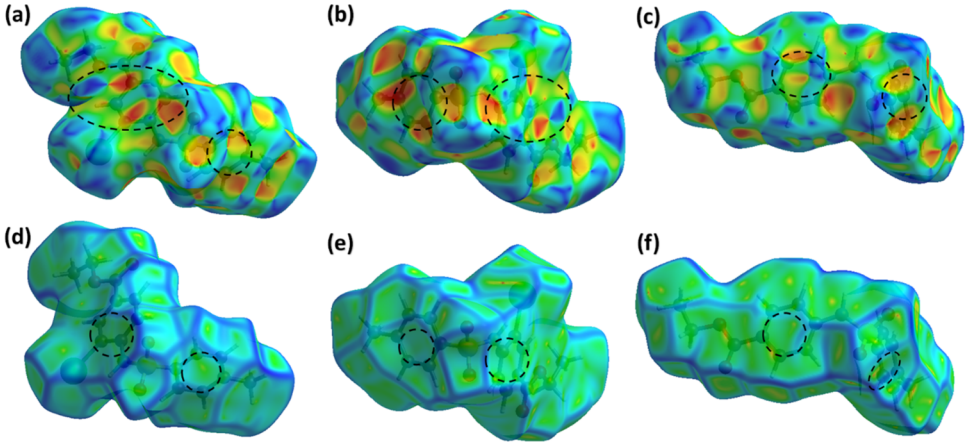

Figure 5. Hirshfeld surface plotted over the shape index in the range of −1 to 1 au, for (a) **MSBT**, (b) **MSBM**, and (c) **DAYWUW**. Hirshfeld surface plotted over curvedness in the range of −4 to −0.4 au, for (d) **MSBT**, (e) **MSBM**, and (f) **DAYWUW**.

always attractive. These two types of energies play prominent roles in defining the total energy between a molecular pair. The interaction energies are calculated for a 3.8 Å cluster around the reference molecule (molecule present in the asymmetric unit), and the HF/3-21G electron density model is used for calculations using TONTOs that is built in software in Crystal Explorer version 21.5. The Coulomb energy is repulsive for a molecular pair with intermolecular distances of 9.69 and 12.16 Å and zero for the molecular pair with an intermolecular distance of 15.48 Å in **MSBT** (Table 4). For **MSBM**, the Coulomb energy is repulsive only for one pair with an intermolecular distance of 9.94 Å (Table S4), whereas in **DAYWUW**, Coulomb energy is not repulsive for any pair (Table S5). The Cartesian coordinates of the atoms that are used for the interaction energy calculations are given in Table S5 for **MSBT**, **MSBM**, and **DAYWUW**, respectively. In the case of **MSBT**, the Coulomb energy is the greatest (negative) for the molecular pair with an intermolecular distance of 7.30 Å, whereas the dispersion energy is the greatest for the molecular pair with an intermolecular distance of 6.20 Å. The corresponding energies for **MSBM** and **DAYWUW** are given in Table S5. The total attractive energy is the greatest for the molecular pair with intermolecular distances of 6.20 Å in **MSBT**, 6.07 Å in **MSBM**, and 7.86 Å in **DAYWUW**. In order to further explore the contribution of Coulomb and dispersion energies in defining the total interaction energy, energy frameworks are constructed. In energy frameworks, the center of the interacting molecules is connected by a cylinder whose width is directly proportional to the strength of the interaction energy. For **MSBT**, **MSBM**, and **DAYWUW**, the width of the cylinder for the energy frameworks of dispersion energy is greater than the width of cylinders for the Coulomb energy (Figure 8), which showed that the dispersion energy is the most significant contributor in defining the total interaction energy in these compounds. We conclude that dispersion energy plays a prominent role in the stabilization of crystal packing.

5.3. DFT Study Results. *5.3.1. Natural Bond Orbital (NBO) Analysis.* Table 5 summarizes NBO charges on the selected atoms of the compounds **MSBT** and **MSBM** (see Figures 1 and 9 for the atom numbering), and Table S8 summarizes the results of the second-order perturbation analysis for them. Analysis of the results in Table 5 shows quite noticeable negative charges on I1 in both compounds,

https://doi.org/10.1021/acsomega.3c04957
ACS Omega 2023, 8, 35307−35320

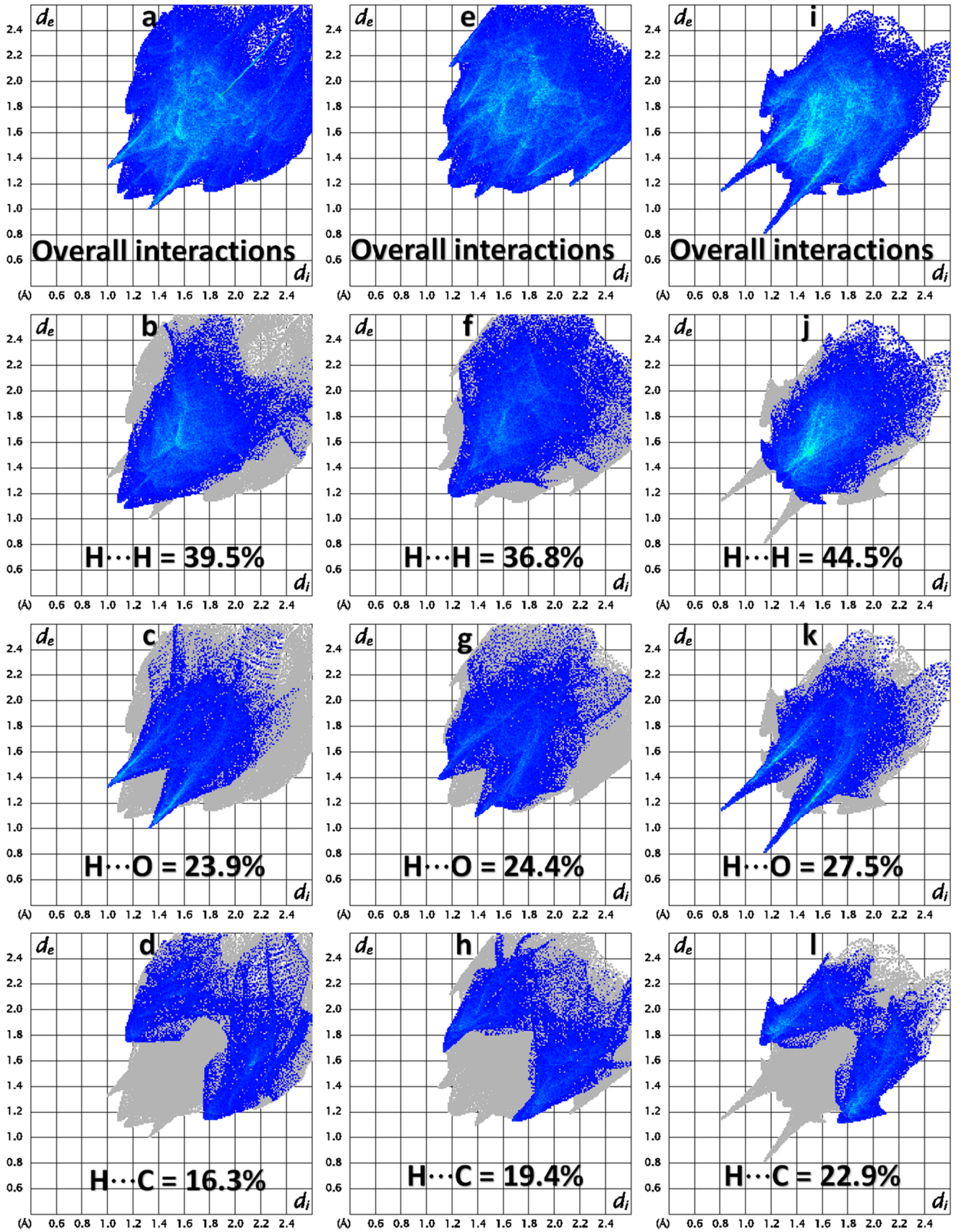

Figure 6. 2D plot of overall interactions and for the important interatomic contacts in the cases of (a−d) **MSBT**, (e−h) **MSBM**, and (i−l) **DAYWUW**.

https://doi.org/10.1021/acsomega.3c04957
ACS Omega 2023, 8, 35307−35320

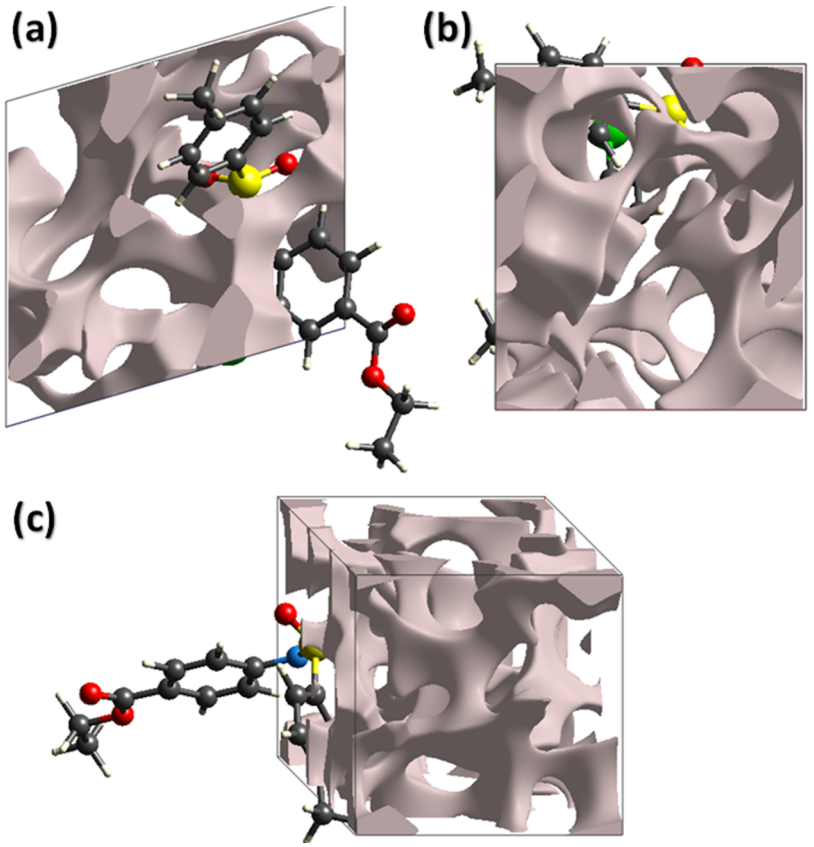

Figure 7. Graphical representations of voids in the crystal packing of (a) **MSBT**, (b) **MSBM**, and (c) **DAYWUW**.

−0.171 to −0.181*e* on N1; −0.175 to −0.261e on the oxygens O1 and O2; −0.278 to −0.281*e* and −0.365 to −0.371*e*, respectively, on the oxygens of the sulfonyl group O3 and O4; −0.472 to −0.474*e* and −0.495 to −0.503*e*, respectively, along with quite noticeable positive charges on S1; 0.818−0.839*e* on the hydrogen bound to N1; 0.148−0.177*e* on the H atoms located close to the O atoms, such as H(C11), 0.155−0.159e; H(C1), 0.114−0.115*e*; H(C8), 0.157−0.183*e*; and H(C5), 0.143−0.148*e*. These results suggest the formation of intramolecular N−H···I bonding and possible C−H···O bonding interactions (cf. C−H···O bond distances in Figure 9 and Tables 2 and 3), along with possible N−H···O−S intramolecular hydrogen-bonding formation (the N−H···O−S bond distances are relatively short, 2.429 and 2.469 for **MSBT** and **MSBM**, respectively; cf. Figure 9a,b). However, it should be noticed that the intramolecular N−H···I bonding in **MSBT** should be stronger than that in **MSBM**, which follows from the longer N−H···I distance in the second compound, 2.865 vs 2.701 Å in **MSBT**, and is further supported by the donor−acceptor interaction analysis (see below). Moreover, these results further suggest formation of various intermolecular interactions, thus supporting the results of the Hirshfeld analysis (see above). It should also be noticed that calculated charges for both compounds are in general quite similar, which is clear due to structure similarities, although some differences can be seen as well (Figure 10).

Next, the results of the NBO second-order perturbation theory analysis (see Table S8) show the presence of various intramolecular donor−acceptor interactions in both compounds. Among these, we can highlight the following donor−acceptor interactions in **MSBT**: between the benzene ring and the ether group, π(C4−C5) → π^*(O2−C3), with stabilization energy 22.10 kcal/mol; within the benzene rings, π(C4−C5) → π^*(C8−C9), π(C6−C7) → π^*(C4−C5), π(C8−C9) → π^*(C6−C7), π(C10−C11) → π^*(C14−C15), π(C12−C13) → π^*(C10−C11), π(C12−C13) → π^*(C14−C15), π(C14−C15) → π^*(C12−C13), with stabilization energies within 20.24−26.13 kcal/mol; interactions involving the carbonyl group, LP(O2) → σ^*(C3−O1) and LP(O2) → σ^*(C3−C4), with stabilization energies 33.65 and 21.04 kcal/mol, respectively; interactions involving the sulfonyl group, LP(O3) → σ^*(S1−C10), LP(O3) → σ^*(S1−O4), and LP(O4) → σ^*(S1−O3), with stabilization energies 20.89, 20.56, and 22.48 kcal/mol, respectively; and interactions within the 2-iodoanilinic group, LP(N1)→ π^*(C6−C7), with stabilization energy 31.77 kcal/mol. Also, it is necessary to mention the relatively weak interaction LP(I1) → σ^*(N1−H(N1)), with a stabilization energy of 1.25 kcal/mol, which supports the formation of the intramolecular N−H···I bonding in **MSBT** (see above).

Next, we can highlight the following donor−acceptor interactions in **MSBM**: within the benzene rings, π(C4−C9) → π^*(C5−C6), π(C5−C6) → π^*(C7−C8), π(C7−C8) → π^*(C4−C9), π(C10−C15) → π^*(C11−C12), π(C13−C14) → π^*(C10−C15), π(C11−C12) → π^*(C13−C14), with energies within 20.57−27.64 kcal/mol; interaction between the benzene ring and the carbonyl group, π(C4−C9) → π^*(O2−C3), with stabilization energy 20.44 kcal/mol; interactions involving the carbonyl group, LP(O1) → π^*(O2−C3), LP(O2) → σ^*(O1−C3), and LP(O2) → σ^*(C3−C4), with stabilization energies within 22.13−54.87 kcal/mol; interactions involving the sulfonyl group, LP(O4) →

https://doi.org/10.1021/acsomega.3c04957
ACS Omega 2023, 8, 35307−35320

Table 4. Interaction Energies between Molecular Pairs in MSBT[a]

										%E_attract	%E_attract	%E_attract
	N	Symop	R	E_ele	E_pol	E_dis	E_rep	E_tot	E_attract	E_ele	E_pol	E_dis
	1	-x, -y, -z	6.20	-21.9	-5.7	-70.2	41.3	-55.7	-97.8	22.4	5.83	71.8
	2	x, y, z	9.69	1.5	-1.8	-26.2	9.2	-15.7	-28	0	6.42	93.4
	2	x, y, z	12.16	3.1	-1.5	-10.2	4.0	-3.8	-11.7	0	12.8	87.2
	1	-x, -y, -z	8.55	-6.1	-3.1	-57.7	21.4	-43.0	-66.9	9.11	4.63	86.2
	1	-x, -y, -z	9.19	-6.8	-0.4	-7.9	16.4	-1.0	-15.1	45	2.65	52.3
	2	x, y, z	12.98	-0.3	-0.3	-5.1	2.4	-3.1	-5.7	5.26	5.26	89.5
	1	-x, -y, -z	8.01	-16.3	-7.4	-17.9	4.1	-34.2	-41.6	39.2	17.8	38.8
	1	-x, -y, -z	9.71	-25.1	-7.8	-21.7	15.8	-37.3	-54.6	45.9	14.3	39.7
	1	-x, -y, -z	7.30	-50.8	-17.6	-43.6	36.0	-73.4	-112	45.4	15.7	39.8
	2	x, y, z	8.89	-7.4	-2.7	-7.2	2.4	-13.9	-17.3	42.8	15.6	41.6
	1	-x, -y, -z	8.56	-2.5	-1.9	-24.2	11.7	-16.0	-28.6	8.74	6.64	84.6
	1	-x, -y, -z	15.02	-1.7	-0.9	-9.7	1.4	-10.0	-12.3	13.8	7.31	78.9
	1	-x, -y, -z	15.48	0.0	-0.1	-6.0	3.5	-2.7	-6.1	0	1.64	98.4

Energy Model	k_ele	k_pol	k_disp	k_rep			
CE-HF ... HF/3-21G electron densities	1.019	0.651	0.901	0.811			

[a]R is the center-to-center distance between the molecules.

σ*(S1−C10), LP(O4) → σ*(S1−O3), and LP(O3) → σ*(S1−O4), with stabilization energies 20.27, 20.80, and 21.86 kcal/mol, respectively; and interactions within the 2-iodoanilinic group, LP(N1)→ π*(C7−C8), with stabilization energy 20.11 kcal/mol. No interaction with LP(I1) → σ*(N1−H(N1)) was found.

Furthermore, it is of interest to compare the NBO energies of intramolecular hydrogen bonding and hydrogen-bonding-like interactions (we classify this way LP(O) → σ*(C−H) interactions) in our compounds with NBO energies of intramolecular hydrogen bonding for several amides considered by Aguilar-Castro et al.[59] In this work, the calculated NBO energies of intramolecular hydrogen bonding are generally within ca. 1−3 kcal/mol, and only two energies are larger, 20.02 and 9.47 kcal/mol. Our results are in quite good agreement with these data, because for the compounds **MSBT** and **MSBM**, the calculated energies of intramolecular hydrogen bonding and hydrogen-bonding-like interactions are generally lower than 5 kcal/mol; see the above as an example of the stabilization energy for the LP(I1) → σ*(N1−H(N1))

https://doi.org/10.1021/acsomega.3c04957
ACS Omega 2023, 8, 35307−35320

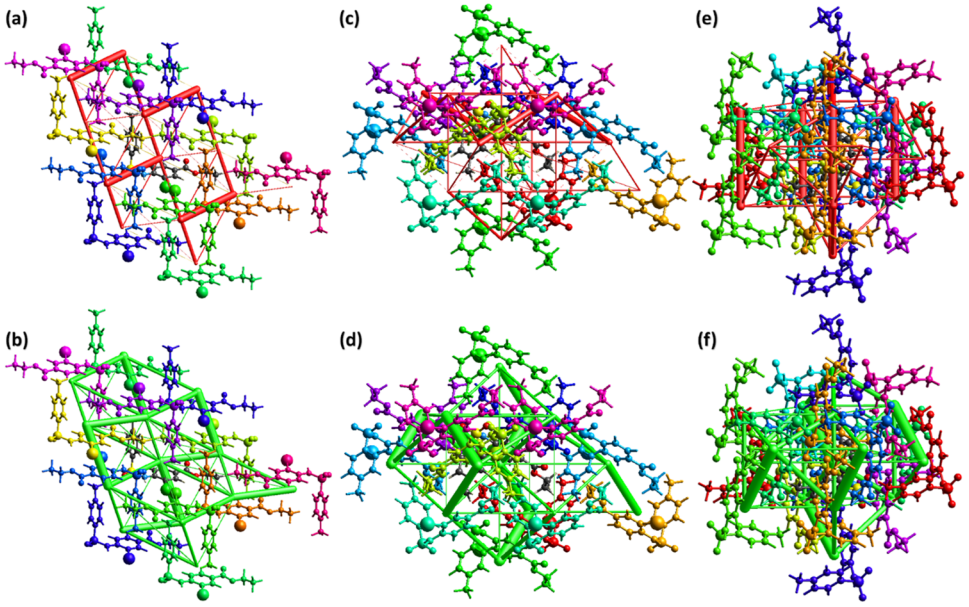

Figure 8. Energy frameworks for (a, b) Coulomb and dispersion energies of **MSBT**, (c, d) Coulomb and dispersion energies of **MSBM**, and (e, f) Coulomb and dispersion energies of **DAYWUW**.

Table 5. Selected NBO Charges, *e*, for the Compounds MSBT and MSBM

						MSBT						
atom	I1	S1	N1	H (N1)	O1	O2	O3	O4	H (C11)	H (C1)	H (C8)	H (C5)
charge, *e*	−0.181	0.818	−0.175	0.148	−0.281	−0.371	−0.472	−0.495	0.155	0.114	0.157	0.148
						MSBM						
atom	I1	S1	N1	H (N1)	O1	O2	O3	O4	H (C11)	H (C1)	H (C8)	H (C5)
charge, *e*	−0.171	0.839	−0.261	0.177	−0.278	−0.365	−0.474	−0.503	0.159	0.115	0.183	0.143

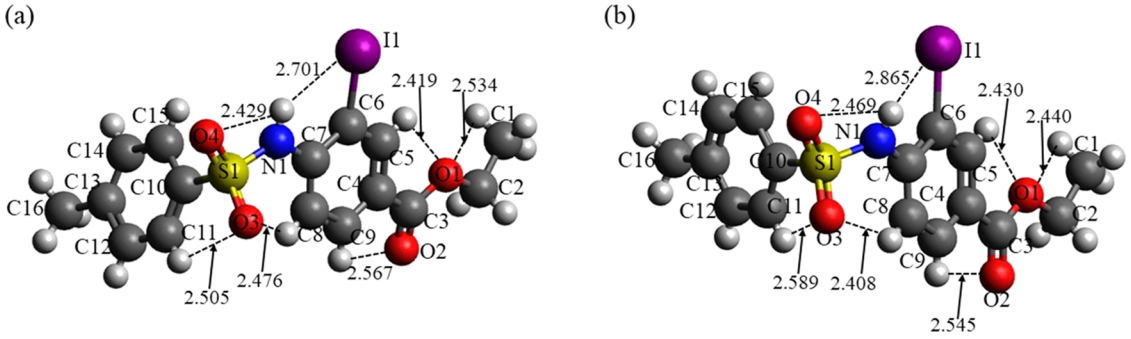

Figure 9. Structures of compounds **MSBT** (a) and **MSBM** (b) with the atom numeration as in Figure 1. The selected interatomic bond distances are given in Å. Color coding is as follows: dark gray for C, light gray for H, lilac for I, red for O, yellow for S, and dark blue for N.

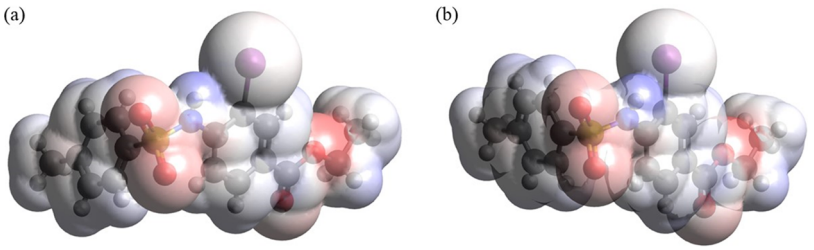

Figure 10. MEP plots for compounds **MSBT** (a) and **MSBM** (b).

interaction, 1.25 kcal/mol. The only stabilization energy for the hydrogen-bonding-like interaction higher than 5 kcal/mol is the energy of the LP(O1) → σ^*(C2-HA(C2)) interaction, 5.25 kcal/mol, for the **MSBT** compound (see Table S8). It is also worth noting that the comparison of the calculated NBO energies of intramolecular hydrogen bonding should be

https://doi.org/10.1021/acsomega.3c04957
ACS Omega 2023, 8, 35307−35320

performed carefully because our compounds are different from the compounds considered by Aguilar-Castro et al.

It should also be noticed that the calculated stabilization energies for both compounds are in general similar, which is clear due to structure similarities, although some noticeable differences can be seen as well.

Thus, as can be seen, the NBO analysis results provide good support for the SC-XRD and Hirshfeld studies, suggesting the formation of both intramolecular and intermolecular interactions for both compounds.

5.3.2. Molecular Electrostatic Potential (MEP) Analysis. Molecular electrostatic potential plots for both compounds are quite similar due to their structural similarities, with negative potential accumulation (as shown by red) occurring on the oxygens of the sulfonyl and carbonyl groups (especially on O1) and positive potential accumulation (as shown by blue) occurring on the N−H group and on the hydrogens connected to C2, C14, and C15. This positive and negative potential accumulation suggests the formation of both intramolecular and intermolecular interactions, thus supporting the results of the SC-XRD and Hirshfeld surface analysis studies.

6. CONCLUSIONS

The orientation of the sulfonamide group plays a key role in determining the crystal shape of substituted aromatic sulfonamides as it can present different kinds of intermolecular attractive forces depending on their orientation. Two polymorphic forms, triclinic (**MSBT**) and monoclinic (**MSBM**) of ethyl 3-iodo-4-((4-methylphenyl)sulfonamido)-benzoate, have been observed. The structure of these polymorphs has been confirmed by a single-crystal analysis. According to SC-XRD analysis, the molecular configuration structures of these polymorphs are stabilized by intramolecular N−H···I and C−H···O bonding together with the offset $\pi\cdots\pi$ stacking interactions between phenyl rings, which are found to be stronger in **MSBM** as compared to **MSBT**. According to Hirshfeld surface analysis, the supramolecular assembly of these polymorphs is mainly stabilized by noncovalent interactions or intermolecular interactions. The NBO and MEP analysis results provide good support for the SC-XRD and Hirshfeld studies, suggesting the presence of both intramolecular and intermolecular interactions in both compounds. The combined experimental and theoretical analysis has found good agreement and indicates good mechanical properties of these polymorphs.

■ ASSOCIATED CONTENT

Supporting Information

The Supporting Information is available free of charge at https://pubs.acs.org/doi/10.1021/acsomega.3c04957.

Processing Summary (CIF)

Processing Summary (CIF)

^{1}H and ^{13}C NMR data of the compound substituted p-toluenesulfonanilide (Figure S1); enrichment ratio of the pair of chemical species in **MSBT** (Table S1), **MSBM** (Table S2), and **DAYWUW** (Table S3); interaction energies between molecular pairs in **MSBM** (Table S4) and **DAYWUW** (Table S5); Cartesian coordinates and occupancy of the atoms of **MSBT** that are used in the interaction energy calculations (Table S6); cartesian coordinates and occupancy of the atoms of **MSBM** that are used in the interaction energy calculations (Table S7); Cartesian coordinates and occupancy of the atoms of **DAYWUW** that are used in the interaction energy calculations (Table S8); and second-order perturbation theory analysis (Table S9) (PDF)

■ AUTHOR INFORMATION

Corresponding Authors

Akbar Ali − *Department of Chemistry, Government College University Faisalabad, 38000 Faisalabad, Pakistan;* orcid.org/0000-0002-2914-0934; Email: akbarchm@gmail.com, akbar.ali@gcuf.edu.pk

Alexander Fernandez de la Torre − *Departamento de Química Orgánica, Facultad de Ciencias Químicas, Universidad de Concepción, Concepción 3801061, Chile;* Email: afndz1982@gmail.com

Authors

Mehreen Riaz − *Department of Applied Chemistry, Government College University Faisalabad, 38000 Faisalabad, Pakistan*

Muhammad Ashfaq − *Department of Physics, University of Sargodha, 40100 Sargodha, Pakistan;* orcid.org/0000-0001-6663-8777

Muhammad Ibrahim − *Department of Applied Chemistry, Government College University Faisalabad, 38000 Faisalabad, Pakistan*

Nadia Akram − *Department of Chemistry, Government College University Faisalabad, 38000 Faisalabad, Pakistan;* orcid.org/0000-0002-4937-2409

Muhammad Nawaz Tahir − *Department of Physics, University of Sargodha, 40100 Sargodha, Pakistan;* orcid.org/0000-0002-6815-9806

Aleksey Kuznetsov − *Departamento de Química, Campus Santiago Vitacura, Universidad Técnica Federico Santa María, Vitacura 7660251, Chile;* orcid.org/0000-0001-8857-3118

Lyanne Rodríguez − *Department of Clinical Biochemistry and Immunohaematology, Thrombosis Research Center, Medical Technology School, Faculty of Health Sciences, Universidad de Talca, Talca 3460000, Chile*

Manal Y. Sameeh − *Chemistry Department, Faculty of Applied Sciences, Al-Leith University College, Umm Al-Qura University, Makkah 24831, Saudi Arabia*

Mohammed A. Assiri − *Research center for Advanced Materials Science (RCAMS), King Khalid University, Abha 61514, Saudi Arabia; Department of Chemistry, Faculty of Science, King Khalid University, Abha 61413, Saudi Arabia*

Complete contact information is available at: https://pubs.acs.org/10.1021/acsomega.3c04957

Notes

The authors declare no competing financial interest.

■ ACKNOWLEDGMENTS

A.F.d.l.T. thanks ANID through the project 'FONDECYT de Iniciacion en Investigation No. 11200057" for the financial support. The authors express their appreciation to the Deanship of Scientific Research at King Khalid University, Saudi Arabia, for this work through the research group program under grant number RGP-2/524/44. Powered@

NLHPC: This research was partially supported by the supercomputing infrastructure of the NLHPC (ECM-02).

REFERENCES

(1) Bernstein, J. *Polymorphism in Molecular Crystals*; Oxford University Press: United Kingdom, 2010; pp 1−424.
(2) IUPAC *Compendium of chemical terminology*, 2nd ed.; (the "Gold Book"), Compiled by McNaught, A. D., Wilkinson, A: Blackwell Scientific Publications, Oxford, United Kingdom, 1997.
(3) Grepioni, F. Themed issue: Polymorphism and crystal forms. *N. J. Chem.* **2008**, *32*, 1657−1658.
(4) Cruz-Cabeza, A. J.; Bernstein, J. Conformational polymorphism. *Chem. Rev.* **2014**, *114*, 2170−2191.
(5) Moore, J. C.; Palmer, R. A.; Yeadon, A. Polymorphism of 4-methyl-2-nitroacetanilide - structure of form-i (white). *Acta Crystallogr., Sect. A* **1978**, *34*, S97.
(6) Moore, J. C.; Yeadon, A.; Palmer, R. A. Crystal and molecular structures of two polymorphs of 4-methyl-2-nitroacetanilide (MNA). *J. Crystallogr. Spectrosc. Res.* **1983**, *13*, 279−292.
(7) Moore, J. C.; Yeadon, A.; Palmer, R. A. Crystal and molecular structure of an amber polymorph of 4-methyl-2-nitroacetanilide (MNA). *J. Crystallogr. Spectrosc. Res.* **1984**, *14*, 283−291.
(8) Demartin, F.; Filippini, G.; Gavezzotti, A.; Rizzato, S. X-ray diffraction and packing analysis on vintage crystals: Wilhelm Koerner's nitrobenzene derivatives from the School of Agricultural Sciences in Milano. *Acta Crystallogr., Sect. B: Struct. Sci.* **2004**, *60*, 609−620.
(9) Beran, G. J. O.; Wright, S. E.; Greenwell, C.; Cruz-cabeza, A. The interplay of intra- and intermolecular errors in modeling conformational polymorphs. *J. Chem. Phys.* **2022**, *156*, No. 104112.
(10) (a) Nyman, J.; Yu, L.; Reutzel-Edens, S. M. Accuracy and reproducibility in crystal structure prediction: the curious case of ROY. *CrystEngComm* **2019**, *21*, 2080−2088. (b) Funnell, N. P.; Bull, C. L.; Ridley, C. J.; Capelli, S. Structural behaviour of OP-ROY at extreme conditions. *CrystEngComm* **2019**, *21*, 4473−4483. (c) Gushurst, K. S.; Nyman, J.; Boerrigter, S. X. M. The PO13 crystal structure of ROY. *CrystEngComm* **2019**, *21*, 1363−1368. (d) Harty, E. L.; Ha, A.R.; Warren, M.R.; Thompson, A.L.; Allan, D.R.; Goodwin, A.L.; Funnell, N.P. Reversible piezochromism in a molecular wine-rack. *Chem.Commun.* **2015**, *51*, 10608−10611.
(11) Li, H.; Stowell, J. G.; Borchardt, T. B.; Byrn, S. R. Synthesis, Conformational Polymorphism, and Construction of a G−T Diagram of 2-[(2-Nitrophenyl)amino]-3-thiophenecarbonitrile. *Cryst. Growth Des.* **2006**, *6*, 2469−2474.
(12) Li, X.; Ou, X.; Wang, B.; Rong, H.; Wang, B.; Chang, C.; Shi, B.; Yu, L.; Lu, M. Rich polymorphism in nicotinamide revealed by melt crystallization and crystal structure prediction. *Commun. Chem* **2020**, *3*, No. 152, DOI: 10.1038/s42004-020-00401-1.
(13) Sanphui, P.; Sarma, B.; Nangia, A. Polymorphism in secondary benzene sulfonamides. *Cryst. Growth Des.* **2010**, *10*, 4550−4564.
(14) Roy, S.; Nangia, A. Kinetic and Thermodynamic Conformational Polymorphs of Bis(p-tolyl) Ketone p-Tosylhydrazone: The Curtin−Hammett Principle in Crystallization. *Cryst. Growth Des.* **2007**, *7*, 2047−2058.
(15) Terada, S.; Katagiri, K.; Masu, H.; Danjo, H.; Sei, Y.; Kawahata, M.; Azumaya, I.; et al. Polymorphism of aromatic sulfonamides with fluorine groups. *Cryst. Growth Des.* **2012**, *12*, 2908−2916.
(16) (a) Ali, A.; Khalid, M.; Rehman, M. F. U.; Haq, S.; Ali, A.; Tahir, M. N.; Ashfaq, M.; Rasool, F.; Braga, A. A. C. Efficient Synthesis, SC-XRD, and theoretical studies of O-Benzenesulfonylated pyrimidines: Role of noncovalent Interaction Influence in Their supramolecular network. *ACS Omega* **2020**, *5*, 15115−15128. (b) Khalid, M.; Ali, A.; Abid, S.; Tahir, M. N.; Khan, M. U.; Ashfaq, M.; Imran, M.; Ahmad, A. Facile Ultrasound-Based Synthesis, SC-XRD, DFT exploration of the substituted Acyl-hydrazones: An experimental and theoretical slant towards supramolecular chemistry. *ChemistrySelect* **2020**, *5*, 14844−14856. (c) Khalid, M.; Ali, A.; De la Torre, A. F.; Marrugo, K. P.; Concepcion, O.; Kamal, G. M.; Muhammad, S.; Al-Sehemi, A. G. Facile Synthesis, spectral (IR, Mass, UV@Vis, NMR), Linear and nonlinear Investigation of the novel phosphonate compounds: A combined experimental and simulation study. *ChemistrySelect* **2020**, *5*, 2994−3006.
(17) Maharramov, A. M.; Mahmudov, K. T.; Kopylovich, M. N.; Pombeiro, A. J. *Non-covalent Interactions in the Synthesis and Design of New Compounds*; Wiley Online Library, 2016.
(18) (a) Li, S.; Bu, R.; Gou, R.-j.; Zhang, C. Hirshfeld surface method and Its application in energetic crystals. *Cryst. Growth Des.* **2021**, *21* (12), 6619−6634. (b) Spackman, M. A.; Jayatilaka, D. Hirshfeld surface analysis. *CrystEngComm* **2009**, *11*, 19−32. (c) Ali, A.; Din, Z. U.; Ibrahim, M.; Ashfaq, M.; Muhammad, S.; Gull, D.; Tahir, M. N.; Rodrigues-Filho, E.; Al-Sehemi, A. G.; Suleman, M. Acid catalyzed one-pot approach towards the synthesis of curcuminoid systems: unsymmetrical diarylidene cycloalkanones, exploration of their single crystals, optical and nonlinear optical properties. *RSC Adv.* **2023**, *13*, 4476. (d) Ashfaq, M.; Ali, A.; Tahir, M. N.; Kuznetsov, A.; Munawar, K. S.; Muhammad, S. Synthesis, single-crystal exploration, hirshfeld surface analysis, and DFT investigation of the thiosemicarbazones. *J. Mol. Struct.* **2022**, *1262*, No. 133088. (e) Ashfaq, M.; Khalid, M.; Tahir, M. N.; Ali, A.; Arshad, M. N.; Asiri, A. M. Synthesis of crystalline fluoro-functionalized Imines, single crystal investigation, Hirshfeld surface analysis, and theoretical exploration. *ACS Omega* **2022**, *7*, 9867−9878. (f) Ali, A.; Ashfaq, M.; Din, Z. U.; Ibrahim, M.; Khalid, M.; Assiri, M. A.; Riaz, A.; Tahir, M. N.; Rodrigues-Filho, E.; Imran, M.; Kuznetsov, A. Synthesis, structural, and intriguing electronic properties of symmetrical Bis-Aryl-α,β-unsaturated ketone derivatives. *ACS Omega* **2022**, *7*, 39294−39309.
(19) Mohandas, T.; Inbaseelan, C. R. D.; Saravanan, S.; Sakthivel, P. Glycine−D-tartaric acid (1/1). *Acta Crystallogr., Sect. E: Struct. Rep. Online* **2013**, *69*, No. 236.
(20) Sanz, R.; Martínez, F.; Orcajo, G.; Wojtas, L.; Briones, D. Synthesis of a honeycomb-like Cu-based metal−organic framework and its carbon dioxide adsorption behavior. *Dalton Trans.* **2013**, *42*, 2392−2398.
(21) Sheldrick, G. M. A short history of SHELX. *Acta Crystallogr., Sect. A: Found. Crystallogr.* **2008**, *64*, 112−122.
(22) Kratzert, D.; Holstein, J.J.; Krossing, I. DSR: enhanced modelling and refinement of disordered structures with SHELXL. *J. Appl. Crystallogr.* **2015**, *48*, 933−938.
(23) Chuchuryukin, A. V.; Huang, R.; Lutz, M.; Chadwick, J. C.; Spek, A. L.; van Koten, G. NCN-pincer metal complexes (Ti, Cr, V, Zr, Hf, and Nb) of the phebox ligand (S, S)-2, 6-bis (4′-isopropyl-2′-oxazolinyl) phenyl. *Organometallics* **2011**, *30*, 2819−2830.
(24) Macrae, C. F.; Sovago, I.; Cottrell, S.J.; Galek, P.T.; McCabe, P.; Pidcock, E.; Platings, M.; Shields, G.P.; Stevens, J.S.; Towler, M.; Wood, P. A. Mercury 4.0: From visualization to analysis, design and prediction. *J. Appl. Crystallogr.* **2020**, *53*, 226−235.
(25) Farrugia, L. J. WinGX and ORTEP for Windows: an update. *J. Appl. Crystallogr.* **2012**, *45*, 849−854.
(26) (a) da Silva, G. P.; Ali, A.; da Silva, R. C.; Jiang, H.; Paixao, M. W. Tris (trimethylsilyl) silane and visible-light irradiation: a new metal-and additive-free photochemical process for the synthesis of indoles and oxindoles. *Chem. Commun.* **2015**, *51*, 15110−15113. (b) Bressy, C.; Alberico, D.; Lautens, M. A route to annulated indoles via a palladium-catalyzed tandem alkylation/direct arylation reaction. *J. Am. Chem. Soc.* **2005**, *127*, 13148−13149.
(27) Frisch, M. J.; Trucks, G. W.; Schlegel, H. B.; Scuseria, G. E.; Robb, M. A.; Cheeseman, J. R.; Scalmani, G.; Barone, V.; Mennucci, B.; Petersson, G. A.; Nakatsuji, H.; Caricato, M.; Li, X.; Hratchian, H. P.; Izmaylov, A. F.; Bloino, J.; Zheng, G.; Sonnenberg, J. L.; Hada, M.; Ehara, M.; Toyota, K.; Fukuda, R.; Hasegawa, J.; Ishida, M.; Nakajima, T.; Honda, Y.; Kitao, O.; Nakai, H.; Vreven, T.; Montgomery, J. A., Jr; Peralta, J. E.; Ogliaro, F.; Bearpark, M.; Heyd, J. J.; Brothers, E.; Kudin, K. N.; Staroverov, V. N.; Kobayashi, R.; Normand, J.; Raghavachari, K.; Rendell, A.; Burant, J. C.; Iyengar, S. S.; Tomasi, J.; Cossi, M.; Rega, N.; Millam, J. M.; Klene, M.; Knox, J. E.; Cross, J. B.; Bakken, V.; Adamo, C.; Jaramillo, J.; Gomperts, R.; Stratmann, R. E.; Yazyev, O.; Austin, A. J.; Cammi, R.; Pomelli, C.;

https://doi.org/10.1021/acsomega.3c04957
ACS Omega 2023, 8, 35307−35320

Ochterski, J. W.; Martin, R. L.; Morokuma, K.; Zakrzewski, V. G.; Voth, G. A.; Salvador, P.; Dannenberg, J. J.; Dapprich, S.; Daniels, A. D.; Farkas, Ö.; Foresman, J. B.; Ortiz, J. V.; Cioslowski, J.; Fox, D. J. *Gaussian 16*, revision 01,B; Gaussian, Inc.: Wallingford CT, 2016.
(28) Becke, A. D. Density-functional thermochemistry. III. The role of exact exchange. *J. Chem. Phys.* **1993**, *98*, 5648−5652.
(29) Weigend, F.; Ahlrichs, R. Balanced basis sets of split valence, triple zeta valence and quadruple zeta valence quality for H to Rn: Design and assessment of accuracy. *Phys. Chem. Chem. Phys.* **2005**, *7*, 3297−3305.
(30) Weigend, F. Accurate coulomb-fitting basis sets for H to Rn. *Phys. Chem. Chem. Phys.* **2006**, *8*, 1057−1065.
(31) Dobbs, K. D.; Hehre, W. J. Molecular-orbital theory of the properties of inorganic and organometallic compounds. 4. Extended basis-sets for 3rd row and 4th row, main-group elements. *J. Comput. Chem.* **1986**, *7*, 359−378.
(32) Tomasi, J.; Mennucci, B.; Cammi, R. Quantum mechanical continuum solvation models. *Chem. Rev.* **2005**, *105*, 2999−3093.
(33) Reed, A. E.; Curtiss, L. A.; Weinhold, F. Intermolecular interactions from a natural bond orbital, donor-acceptor viewpoint. *Chem. Rev.* **1988**, *88*, 899−926.
(34) Hanwell, M. D.; Curtis, D. E.; Lonie, D. C.; Vandermeersch, T.; Zurek, E.; Hutchison, G. R. Avogadro: an advanced semantic chemical editor, visualization, and analysis platform. *J. Cheminf.* **2012**, *4*, 1−17.
(35) Avogadro: an open-source molecular builder and visualization tool. Version 1.1.1. http://avogadro.cc/.
(36) Xing, J. D.; Nan, Z. H. N-[4-(Ethoxycarbonyl) phenyl]-p-tolylsulfonamide. *Acta Crystallogr., Sect. E: Struct. Rep. Online* **2005**, *61*, 4320−4321.
(37) Sohail, M.; Asghar, M. N.; Tahir, M. N.; Shafique, M.; Ashfaq, M. Methyl 4-{[(4-methylphenyl)sulfonyl] amino} benzoate. *Acta Crystallogr., Sect. E: Struct. Rep. Online* **2012**, *68*, 666.
(38) Nan, Z. H.; Xing, J. D. 4-(Tosylamino) benzoic acid. *Acta Crystallogr., Sect. E: Struct. Rep. Online* **2006**, *62*, 1978−1979.
(39) Spackman, P. R.; Turner, M.J.; McKinnon, J.J.; Wolff, S.K.; Grimwood, D.J.; Jayatilaka, D.; Spackman, M.A. Crystalexplorer: A program for Hirshfeld surface analysis, visualization and quantitative analysis of molecular crystals. *J. Appl. Crystallogr.* **2021**, *54*, 1006−1011.
(40) Spackman, M.A.; Jayatilaka, D. Hirshfeld surface analysis. *CrystEngComm* **2009**, *11*, 19−32.
(41) Haroon, M.; Baig, M.W.; Akhtar, T.; Tahir, M.N.; Ashfaq, M. Relativistic two-component time dependent density functional studies and Hirshfeld surface analysis of halogenated arylidenehydrazinylthiazole derivatives. *J. Mol. Struct.* **2023**, *1287*, No. 135692.
(42) Malik, A. N.; Kuznetsov, A.; Ali, A.; Ashfaq, M.; Tahir, M.N.; Siddique, A. Imine-based Zwitterion: Synthesis, single-crystal characterization, and computational investigation. *J. Mol. Struct.* **2022**, *1253*, No. 1253132237.
(43) Zainab, S.; Siddiqui, W.A.; Raza, M.A.; Ashraf, A.; Pervaiz, M.; Ali, F.; Younas, U.; Saleem, A.; Ashfaq, M.; Tahir, M.N. Synthesis, characterization, crystal structure, Hirshfeld surface analysis and DFT of 1,2-benzothiazine metal (II) complexes. *J. Mol. Struct.* **2023**, *1284*, No. 135316.
(44) Ali, A.; Khalid, M.; Tahir, M.N.; Imran, M.; Ashfaq, M.; Hussain, R.; Assiri, M.A.; Khan, I. Synthesis of diaminopyrimidine sulfonate derivatives and exploration of their structural and quantum chemical insights via SC-XRD and the DFT approach. *ACS Omega* **2021**, *6*, 7047−7057.
(45) (a) Spackman, M. A.; Jayatilaka, D. Hirshfeld surface analysis. *CrystEngComm* **2009**, *11*, 19−32. (b) Saeed, A.; Ashraf, S.; Flörke, U.; Delgado Espinoza, Z. Y.; Erben, M. F.; Pérez, H. Supramolecular self-assembly of a coumarine-based acylthiourea synthon directed by π-stacking interactions: Crystal structure and Hirshfeld surface analysis. *J. Mol. Struct.* **2016**, *1111*, 76−83.
(46) McKinnon, J. J.; Jayatilaka, D.; Spackman, M. A. Towards quantitative analysis of intermolecular interactions with Hirshfeld surfaces. *Chem. Commun.* **2007**, *37*, 3814−3816, DOI: 10.1039/b704980c.
(47) Ashfaq, M.; Tahir, M. N.; Muhammad, S.; Munawar, K. S.; Ali, S.; Ahmed, G.; Al-Sehemi, A. G.; Alarfaji, S. S.; Ibraheem, M. E. Shedding light on the synthesis, crystal structure, characterization, and computational study of optoelectronic properties and bioactivity of imine derivatives. *ACS Omega* **2022**, *7*, 5217−5230.
(48) Ashfaq, M.; Tahir, M. N.; Kuznetsov, A.; Mirza, S. H.; Khalid, M.; Ali, A. DFT and single crystal analysis of the pyrimethamine-based novel co-crystal salt: 2,4-diamino-5-(4-chloro-phenyl)-6-ethyl-pyrimidin-1-ium:4-hydroxybenzoate:methanol:hydrate (1:1:1:1) (DEHMH). *J. Mol. Struct.* **2020**, *1199*, No. 127041.
(49) Tahir, M. N.; Ali, A.; Khalid, M.; Ashfaq, M.; Naveed, M.; Murtaza, S.; Shafiq, I.; Asghar, M. A.; Orfali, R.; Perveen, S. Efficient synthesis of imine-carboxylic acid functionalized compounds: single crystal, Hirshfeld surface and quantum chemical exploration. *molecules* **2023**, *28*, 2967−2984.
(50) Jelsch, C.; Ejsmont, K.; Huder, L. The enrichment ratio of atomic contacts in crystals, an indicator derived from the Hirshfeld surface analysis. *IUCrJ* **2014**, *1*, 119−128.
(51) Faihan, A. S.; AlShammari, R. H.; Ashfaq, M.; Muhammad, S.; Al-Jibori, S. A.; Tahir, M. N.; Hatshan, M. R.; Al-Janabi, A. S.; Al-Moayid, S. M. Synthesis, spectroscopic, crystallographic, quantum and molecular docking investigations of cis-4,5-diphenylimidazolidine-2-thione. *J. Mol. Struct.* **2023**, *1286*, No. 135633, DOI: 10.1016/j.molstruc.2023.135633.
(52) Turner, M. J.; McKinnon, J.J.; Jayatilaka, D.; Spackman, M.A. Visualisation and characterisation of voids in crystalline materials. *CrystEngComm* **2011**, *13*, 1804−1813.
(53) Ali, A.; Khalid, M.; Ashfaq, M.; Malik, A. N.; Tahir, M. N.; Assiri, M. A.; Imran, M.; de AlcântaraMorais, S. F.; Braga, A. A. C. Preparation, QTAIM and single-crystal exploration of the pyrimethamine-based co-crystal salts with substituted benzoic acids. *ChemistrySelect* **2022**, *7*, No. e202200349, DOI: 10.1002/slct.202200349.
(54) Askerov, R. K.; Ashfaq, M.; Chipinsky, E. V.; Osmanov, V. K.; Tahir, M. N.; Baranov, E. V.; Fukin, G. K.; Khrustalev, V. N.; Nazarov, R. H.; Borisova, G. N.; Matsulevich, Z. V.; Maharramov, A. M.; Borisov, A. V. Synthesis, crystal structure, exploration of the supramolecular assembly through Hirshfeld surface analysis and bactericidal activity of the cadmium organometallic complexes obtained from the heterocyclic ligand. *Results Chem.* **2022**, *4*, No. 100600, DOI: 10.1016/j.rechem.2022.100600.
(55) Turner, M. J.; Grabowsky, S.; Jayatilaka, D.; Spackman, M. A. Accurate and efficient model energies for exploring intermolecular interactions in molecular crystals. *J. Phys. Chem. Lett.* **2014**, *5*, 4249−4255.
(56) Turner, M. J.; Thomas, S. P.; Shi, M. W.; Jayatilaka, D.; Spackman, M. A. Energy frameworks: insights into interaction anisotropy and the mechanical properties of molecular crystals. *Chem. Commun.* **2015**, *51*, 3735−3738.
(57) Kurbanova, M.; Ashfaq, M.; Tahir, M. N.; Maharramov, A.; Dege, N.; Koroglu, A. Synthesis, crystal structure, supramolecular assembly exploration by Hirshfeld surface analysis and computational study of 6-bromo-2-oxo- 2H-chromene-3-carbonitrile (BOCC). *J. Struct. Chem.* **2023**, *64* (2), 302−312.
(58) Kurbanova, M.; Ashfaq, M.; Tahir, M. N.; Maharramov, A.; Dege, N.; Ramazanzade, N.; Cinar, E. B. Synthesis, crystal Structure, supramolecular assembly inspection by hirshfeld surface analysis and computational exploration of 4-Phenyl-6-(p-Tolyl)Pyrimidin-2 (1H)-One (PPTP). *J. Struct. Chem.* **2023**, *64*, 437−449.
(59) Aguilar-Castro, L.; Tlahuextl, M.; Mendoza-Huizar, L.H.; Tapia-Benavides, A. R.; Tlahuext, H. Hydrogen bond studies in substituted N-(2-hydroxyphenyl)-2-[(4-methylbenzenesulfonyl)-amino]acetamides. *ARKIVOC* **2008**, 210−226.

https://doi.org/10.1021/acsomega.3c04957
ACS Omega 2023, 8, 35307−35320